An Adaptive Overcurrent Protection Scheme for Distribution Networks

F. Coffele, C. Booth, and A. Dyśko, *Member, IEEE*

***Abstract*—Distribution networks are evolving toward the vision of smart grids, with increasing penetration of distributed generation (DG), introduction of active network management (ANM), and potentially islanded modes of operation. These changes affect fault levels and fault current paths and have been demonstrated to compromise the correct operation of the overcurrent protection system. This paper presents an adaptive overcurrent protection system which automatically amends the protection settings of all overcurrent relays in response to the impact of DG, ANM, and islanding operation. The scheme has been developed using commercially available protection devices, employs IEC61850-based communications, and has been demonstrated and tested using a hardware-in-the-loop laboratory facility. A systematic comparison of the performance of the proposed adaptive scheme alongside that of a conventional overcurrent scheme is presented. This comparison quantifies the decrease in false operations and the reduction of mean operating time that the adaptive system offers.**

***Index Terms*—Adaptive protection, distributed generation (DG), islanded operation, network automation, time overcurrent protection.**

I. Introduction

THE ONGOING increase in the penetration of distributed generation (DG) and the adoption of active network-management (ANM) solutions in distribution networks throughout the world creates a network protection challenge due to the effects on fault levels and fault current paths.

DG introduces an additional source of fault current, which may increase the total fault level within the network, while possibly altering the magnitude and direction of the fault currents seen by specific protection relays. The contribution of one single generating unit is normally not large, but the aggregate effect of many generating units can have a significant impact on fault currents and affect the operation of the overcurrent protection system [1].

ANM solutions, which have been introduced to manage DG, energy storage, loads, circuit breakers (CBs), and switches to allow voltage control, power-flow management, demand-side management, automatic restoration, and minimization of power system losses, also affect the fault levels and the fault current paths [2].

Furthermore, as the penetration of DG increases, the islanded operation of certain sections of the distribution network may become beneficial and increase the reliability of the power supply to the customers [3]. However, changing between the islanded and grid-connected modes of operation creates two scenarios with very different fault levels [4].

The combination of DG, ANM, and the potential for islanded operation results in network conditions where fault levels and fault current paths change by disturbing the operation of the overcurrent relays (OCRs). The authors of [1], [5]–[8] showed that DG affects the sensitivity and the operating time of the OCRs while the authors of [9] proved that changes in network topology compromise the correct coordination between OCRs. The impact of islanding was analyzed in [4] and [10], where the authors assessed the amount of fault-level reduction during islanded operation and proved that it causes slow operating times and possible blinding of OCRs.

Solutions to the impact of DG have been presented in [11] where the authors suggest adopting distance protection, in [12]–[14] where the authors propose using fault current limiters (FCLs), and in [14]–[16] where the authors suggest using adaptive protection. The authors of [14] and [15] have proposed using sets of protection settings—one for DG connected and one for the DG not connected to the network, while the authors of [16] have proposed a scheme where the settings of overcurrent protection relays are amended in real time based on the fault level and the DG connection status. A solution that caters for islanded operation has been proposed in [10] and [17], where the authors demonstrate how a simple adaptive overcurrent protection scheme with two setting groups—one for grid connected and one for islanded mode of operation may solve the problem. It appears that, as yet, no solution has been proposed to address the impact of ANM systems on network protection.

All of the proposed adaptive overcurrent protection systems in the literature seem to concentrate on the solution to a specific protection performance problem and disregard other aspects of future networks that may impact performance. Therefore, these schemes are somewhat limited, as in the future, it is likely that DG, ANM, and islanded operation will all be factors that will impact protection.

Accordingly, this paper presents an adaptive overcurrent protection scheme that addresses all of these issues simultaneously. The main difficulty in developing a solution to the aggregated problems caused by DG, ANM, and islanding is that the number of possible network conditions is very large and it becomes unfeasible to precalculate protection settings

Manuscript received July 25, 2013; revised November 01, 2013; accepted December 04, 2013. This work was supported in part by the UK Research Councils' Energy Programme as part of the Supergen FlexNet Consortium under-Grant EP/E04011X/1. Paper no. TPWRD-00837-2013.

F. Coffele was with the Department of Electronic and Electrical Engineering. He is now with the Power Networks Demonstration Centre, University of Strathclyde, Glasgow, G68 0EF, U.K.

C. Booth and A. Dyśko are with the Department of Electronic and Electrical Engineering, University of Strathclyde, Glasgow G1 1XW, U.K. (e-mail: federico.coffele@strath.ac.uk; campbell.d.booth@strath.ac.uk; a.dysko@strath.ac.uk).

Digital Object Identifier 10.1109/TPWRD.2013.2294879

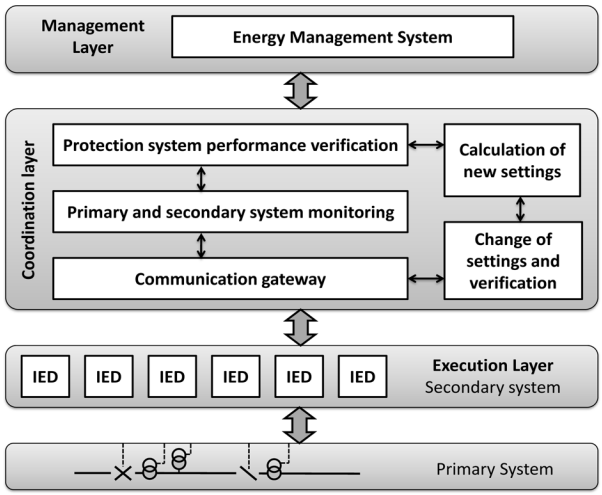

Fig. 1. Adaptive overcurrent protection system architecture.

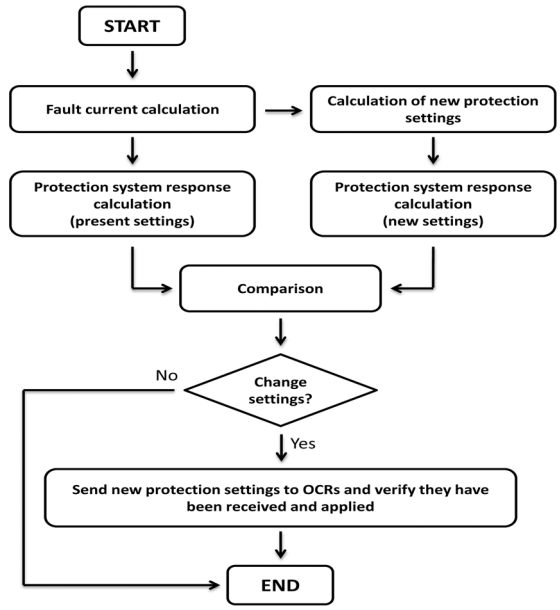

Fig. 2. Adaptive overcurrent protection algorithm.

and establish a manageable number of setting groups which would cover all potential situations. Therefore, the solution proposed in this paper does not use precalculated setting groups but rather establishes the optimum protection settings and applies them to the relays directly whenever there is a significant change in the network, either in terms of DG connectivity, grid connected/islanded status, or changes implemented by an ANM system.

The paper is organized as follows. Section II describes the proposed adaptive overcurrent protection system, its architecture, and its algorithm. Section III presents the test-case distribution network, and Section IV illustrates the hardware-in-the-loop (HIL) simulation environment used to test the proposed solution. Finally, Section V presents the simulation results and, through comparison, quantifies the improvements, in terms of dependability, security, and mean operation time, offered by the adaptive system over a traditional system.

II. Adaptive Overcurrent Protection System

The adaptive overcurrent protection system has been developed using a three-layer architecture illustrated in Fig. 1. The separation of functional layers has been established according to the type of data used and the required response time for each functional group [18].

The primary system is at the foot of the diagram, and includes lines, transformers, DG, circuit breakers (CBs), circuit switches (CSs), current transformers (CTs), voltage transformers (VTs), etc. Directly above this is the execution layer, which includes the intelligent electronic devices (IEDs) installed in the network (e.g., OCRs). The interfaces between the first two layers consist of hardwired links for the provision of measurement data and tripping commands or IEC 61850 process bus communication.

The execution layer is connected to the coordination layer, which is responsible for monitoring and coordinating the IEDs. Finally, at the top, there is an energy-management layer, which is responsible for managing the overall network and communicates with the coordination layer to achieve coordination between adaptive overcurrent protection and ANM. The interface between execution, coordination, and management layers are based on communication protocols, such as DNP3, Modbus, IEC60870-5-103, and IEC61850.

The execution layer is composed of OCRs, receiving measurement data from CTs (and, in some cases, VTs) and tripping CB(s) when faults are detected that should be cleared by the specific OCR(s).

The execution layer is an autonomous layer, that is, the tripping decisions are taken locally using local data without any communication with other layers. This means that in case of communication failure between the execution layer and the coordination layer, the overcurrent protection is not affected. If its settings were to be changed remotely, this would not be possible upon failure of the coordination layer or failure of the communication link between these layers; however, this would not compromise the overcurrent protection system but would mean that the protection settings are not optimized until the communication is restored.

The implementation of the adaptive protection system is facilitated with the introduction of enhanced functionality to the coordination layer, which includes additional functions that are not present in a traditional protection system. Fig. 2 presents the algorithm of the developed adaptive overcurrent protection system.

The algorithm is initiated either by the monitoring block in the coordination layer which reacts to changes in the network, or by the energy-management system which communicates reconfiguration of the network topology, connection-disconnection of DG, and islanded/grid-connected changes.

The adaptive protection system has been implemented using a centralized approach, where setting calculations and modification commands are performed by one processing unit, rather than the agent-based approach, which typically involves the distribution of processing burden and decision making. The reasons why the centralized approach has been adopted are: simpler implementation in real distribution networks where the present supervisory control and data (SCADA) is centralized, easier commissioning, and validation of the centralized solution when it is compared to the agent-based solution.

The following sections explain the individual components of the adaptive overcurrent protection algorithm.

A. Fault Current Calculation

Considering the actual network configuration and the status of the DG connection, a series of faults is simulated (usually at the source and remote end of each network section) to calculate the fault current measured by the OCRs for each fault scenario. A program, written in Python 2.7 [19], accesses the IPSA Power [20] fault calculation tool through its application program interface (API), simulates the faults (through instructing IPSA to execute the appropriate simulations), and saves the fault currents that would be measured by each protection device for every simulated fault. These are saved to a fault current matrix F

$$\mathbf{F} = \begin{bmatrix} I_{f11} & \cdots & I_{f1m} \\ \vdots & \ddots & \vdots \\ I_{fn1} & \cdots & I_{fnm} \end{bmatrix} \tag{1}$$

where n is the number of protection devices and m is the number of simulated faults.

B. Calculation of New Protection Settings

New protection settings are calculated considering the present configuration of the network. All OCRs' settings are calculated in a "downstream to upstream" fashion, that is, starting from the high-voltage (HV)/low-voltage (LV) transformers' fixed fuse current/time characteristics.

This approach is different from the common approach used by distribution network operators (DNOs) to calculate the protection settings because DNOs normally calculate the protection settings starting from upstream, that is, grading from the protections at higher voltages and moving downstream; and favors one set of protection settings which would be applicable to all different network configurations. The reason why the downstream to upstream calculation method has been adopted instead of the common DNO approach is that it minimizes the protection operating time of the OC protection system for each specific network condition or configuration.

C. Protection System Response Calculation

The protection system response to fault current matrix F is calculated using the prevailing protection settings and the new proposed protection settings as calculated in Section II-B. The results are saved in the operating time matrices $\mathbf{T}^0$ and $\mathbf{T}^1$ for the present settings and the new settings, respectively

$$\mathbf{T}^0 = \begin{bmatrix} t^0_{11} & \cdots & t^0_{1m} \\ \vdots & \ddots & \vdots \\ t^0_{n1} & \cdots & t^0_{nm} \end{bmatrix}; \quad \mathbf{T}^1 = \begin{bmatrix} t^1_{11} & \cdots & t^1_{1m} \\ \vdots & \ddots & \vdots \\ t^1_{n1} & \cdots & t^1_{nm} \end{bmatrix} \tag{2}$$

where n is the number of protection devices being considered; and m is the number of simulated faults.

D. Comparison of Relative Performance and Setting Application Decision

The protection system responses (both with the prevailing settings and the new settings) are analyzed to establish if improvement can be achieved through setting modification. If the new protection settings improve the performance, the decision is made to apply the new settings; otherwise, no further action is taken.

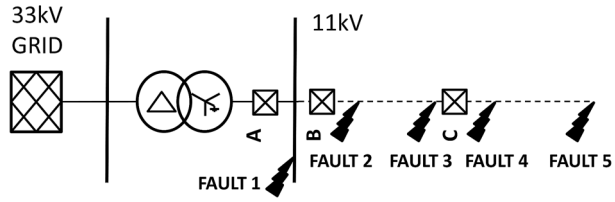

Fig. 3. Fault locations for the protection system-response comparison.

To compare the protection system responses $\mathbf{T}^0$ and $\mathbf{T}^1$, a dedicated algorithm has been designed (implemented in Python 2.7) which analyses both matrices in order to:

1) verify that the operation time of each OCR is within the limits specified in the protection policy;
2) verify the grading margin between protection devices;
3) calculate the mean operation time.

For example, considering a simple circuit in Fig. 3, step 1 verifies that for faults 4 and 5, the operation time of OCR C is shorter than the limits specified in the protection requirements (e.g., an operation time limit of 1 s is typically used in utility protection policies). Step 2 verifies that the difference of the operation time between OCR C and the backup protection OCR B is greater than the minimum grading margin specified in the protection requirements (a sample grading margin is 0.3 s in a typical utility protection policy).

Steps 1 and 2 are repeated for a series of simulated faults at different locations (the source and remote end of each feeder section) as shown in Fig. 3.

The first two steps have higher priority with respect to the third step; therefore, if $\mathbf{T}^1$ does not pass the two verification steps, but $\mathbf{T}^0$ does, the proposed new settings are discarded, while if $\mathbf{T}^0$ does not pass the two verification steps and $\mathbf{T}^1$ does, the proposed new settings are applied, without the third verification step.

If $\mathbf{T}^0$ and $\mathbf{T}^1$ pass the first and the second verification, the third step is the comparison of the mean operation times obtained from $\mathbf{T}^0$ and $\mathbf{T}^1$ according to

$$\mathrm{t}^0_{\mathrm{mean}} = \frac{1}{nm} \sum_{i=1}^{n} \left(\sum_{j=1}^{m} t^0_{ij} \right) \tag{3}$$

$$\mathrm{t}^1_{\mathrm{mean}} = \frac{1}{nm} \sum_{i=1}^{n} \left(\sum_{j=1}^{m} t^1_{ij} \right). \tag{4}$$

Finally, the two mean operation times are compared using (5), and if the condition is satisfied, the new protection settings are applied

$$\mathrm{t}^0_{\mathrm{mean}} - \mathrm{t}^1_{\mathrm{mean}} > \Delta t_m \tag{5}$$

where Δt_m is the minimum difference of the mean times below which the new settings are not applied because the benefit in changing the protection settings would be negligible compared to the risk of fault occurring during the change process.

E. Applying New Protection Settings and Verification

The final step of the algorithm is to send the new protection settings to the OCRs. This is achieved using IEC61850 com-

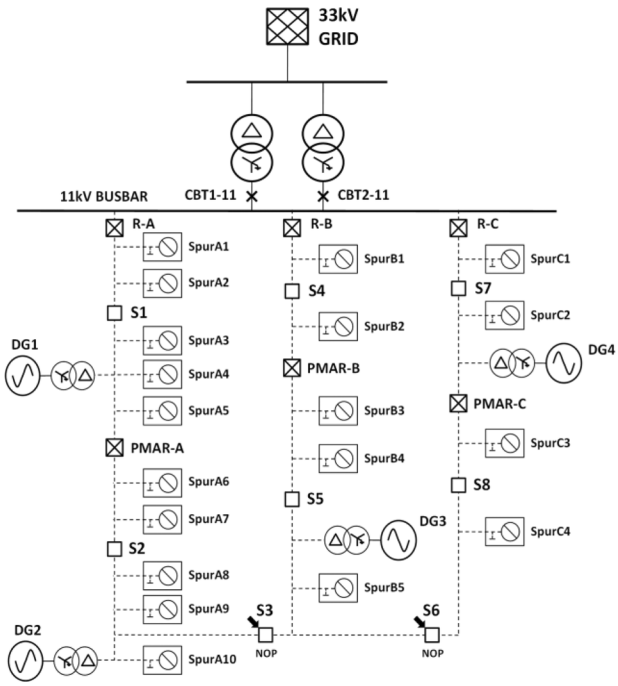

Fig. 4. Distribution network test-case diagram.

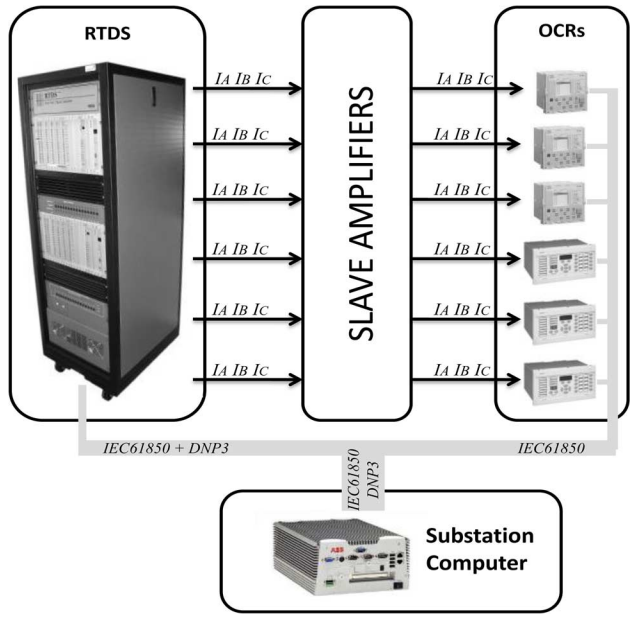

Fig. 5. HIL laboratory testing environment.

munication in two stages. The first stage involves sending the settings, while the second phase involves reading the settings in order to verify that they have been correctly applied.

An IEC61850-compliant protection relay can facilitate two approaches that will enable the application of variable protection settings:

The first approach is based on the employment of protection setting groups. Typically, four or more protection setting groups can be defined, and the adaptive protection system can select the group that represents the closest match to the specific calculated protection settings.

The second approach does not employ predefined protection setting groups. Each specific protection setting (e.g., pick up current, time multiplier, etc.) is accessible for modification, and the adaptive protection system can write the calculated protection settings on an individual basis.

The first approach has the advantage of avoiding the risk of applying wrong protection settings which might cause false tripping or no operation of the protection system during faults while the advantage of the second approach is that it allows more flexibility.

III. Distribution Test-Case Network Model

The test–case network used in this paper is an 11-kV overhead rural distribution network, the "OHA Network," as specified in the United Kingdom Generic Distribution Network (UKGDS) [21]. Fig. 4 depicts the topology of the network which consists of three main feeders and several relatively long spurs.

Both 33/11-kV transformers are rated at 12 MVA, with 8.5% per-unit reactance, delta-star winding configuration, and solid earth connections on the 11-kV side. The lengths of feeders A, B, and C are 8.5, 3.5, and 2.2 km, respectively. Feeder A is rated at 400 A (7.62 MVA), while feeders B and C both have a rating of 250 A (4.76 MVA).

The protection system has been designed to accurately represent present-day networks and adheres to a protection policy that has been supplied by a U.K. distribution network operator (DNO). As shown in Fig. 4, each feeder is protected by a multishot circuit breaker (CB)/recloser at the source end, and by a pole-mounted autorecloser (PMAR) situated at approximately 50% along the feeder. Spurs are connected to the main feeder through spur sectionalizers rather than via fuses, due to the prevailing trend within DNOs to substitute fuses with spur sectionalizers in modern and future distribution networks.

IV. Laboratory Implementation and Simulation

The developed adaptive protection solution has been implemented and demonstrated in an HIL laboratory environment, shown in Fig. 5, in order to verify its effectiveness and compare its performance with a traditional overcurrent protection system.

The real-time digital simulator (RTDS) is used to simulate the primary system behavior in real time during normal and faulty conditions. The output currents of the simulated CTs are amplified using slave amplifiers to inject the OCRs, which operate as if they were connected to a real distribution network and, in the presence of faults, send tripping signals using IEC 61850 GOOSE messaging. The tripping signals are received by the RTDS as an input to the simulation, closing the simulation loop.

A DNP3 master installed on the substation computer is used to communicate with the RTDS to gather periodic status information of CBs, PMARs, network switches, etc. These data are then used by the adaptive overcurrent protection software installed in the substation computer to monitor the network and detect changes which initiate the adaptive algorithm shown in Fig. 2.

When the adaptive protection software is required to change the protection settings of one or more OCRs, this is achieved using an IEC61850-8 master installed in the substation computer to communicate with the OCRs.

TABLE I
NETWORK SCENARIOS

N.	33kV fault level (MVA)	Substation transformers in service	Normally Open Points	DG units in service
1	300	2	S3, S6	No
2	300	2	S1, S6	No
3	300	2	S4, S6	No
4	300	2	S5, S7	No
5	300	2	S3, S6	Yes
6	300	2	S1, S6	Yes
7	300	2	S4, S6	Yes
8	300	2	S5, S7	Yes
9	100	1	S3, S6	Yes
10	100	1	S1, S6	Yes
11	100	1	S4, S6	Yes
12	100	1	S5, S7	Yes
13	NC	NC	S3, S6	Yes
14	NC	NC	S1, S6	Yes
15	NC	NC	S4, S6	Yes
16	NC	NC	S5, S7	Yes

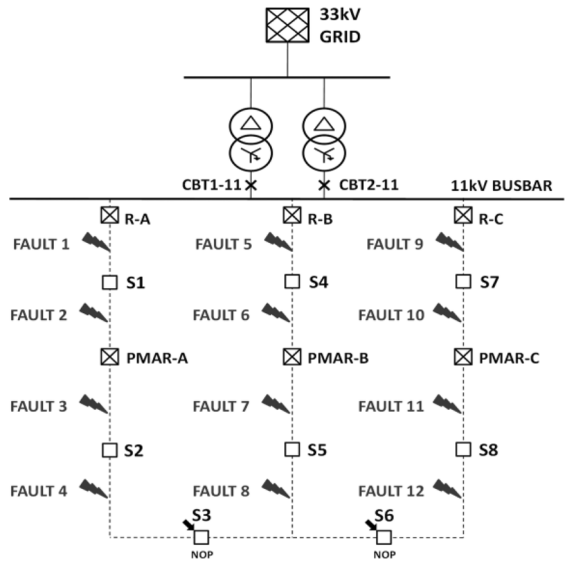

Fig. 6. Fault locations for the HIL simulation.

In order to demonstrate the effectiveness of the developed adaptive overcurrent protection system, a number of scenarios have been simulated (refer to Table I).

The adaptability of the protection system is stimulated by applying various changes to the network configuration. After each change, a set of predefined faults is simulated to verify the protection system performance.

A. Network Scenarios

Scenarios summarized in Table I have been generated to include the following stimuli to the adaptive overcurrent protection system:

- change of fault level due to changes of fault level at 33 kV and the number of in-service transformers at the 33/11-kV distribution substation; normally, both transformers are in operation, but, in some cases, one may be disconnected;
- islanded operation of the 11-kV network, which may be permissible if appropriate DG units are in service;
- change of 11-kV distribution network topology, which can be varied by shifting the normally open points (NOP) as necessary;
- connection/disconnection of the DG units.

B. Fault Simulations

In order to verify the response of the adaptive overcurrent protection system, a series of predefined faults has been simulated for each network scenario, in 12 different fault locations, as shown in Fig. 6.

The faults simulated at each location include:

- 11 phase-to-phase faults with a fault resistance between 0 and 10 Ω (0 Ω, 1 Ω, 2 Ω, etc.);
- 11 phase-to-earth faults with a fault resistance between 0 and 100 Ω (0, 10, 20 Ω, etc.).

All faults have been simulated twice to test the traditional overcurrent protection system and the adaptive overcurrent protection system.

V. SIMULATION RESULTS

The protection system response of the developed adaptive scheme and of the conventional overcurrent protection system with fixed protection settings has been recorded for phase-to-phase and phase-to-earth faults described in Section IV-B.

Fig. 7 shows the measured operating times of the conventional and adaptive overcurrent protection systems for all of the 2112 simulated phase faults. The responses are ordered according to the tripping time starting from the longest. For the first 456 longest faults, the operation of the adaptive overcurrent protection is faster than the conventional IDMT overcurrent protection system, reducing the number of operating times longer than 1 s from 7.15% to 1.81% of the total number of simulated faults.

For all of the other faults, there is no appreciable difference in tripping time, because the delay times of the DTL characteristics are identical. The only exception is for the fault scenarios between 1214 and 1388, where the adaptive overcurrent protection system has a slower tripping time. This is due to the correction of the DTL overcurrent protection settings to guarantee correct coordination between the OCRs when the network topology changes.

Fig. 8 shows the operating time of the conventional and adaptive overcurrent protection system measured for the 2112 simulated earth faults also ordered according to the tripping time and starting from the longest response. Note that as with the phase fault results, the operation of the adaptive protection system is slower for some faults, which is necessary to ensure correct coordination between OCRs as the network topology changes. The increase in operating time is not significant and it is not considered to be a problem since the maximum operating time is 0.572 s. From the results, it is clear that the adaptive protection can be marginally slower in some cases for phase and earth faults. Nevertheless, overall improvement in performance is achieved as coordination problems are avoided by the modification of settings and increased time response to some of the simulated faults.

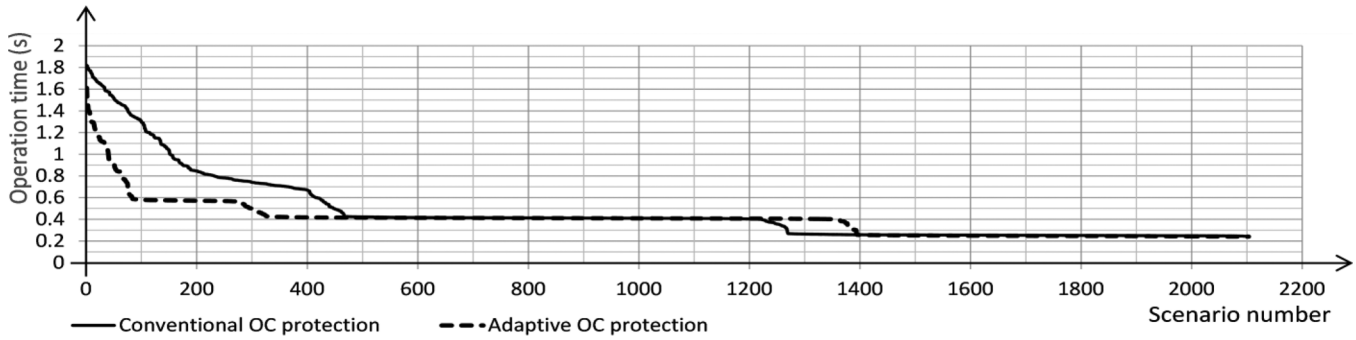

Fig. 7. Measured operating time of conventional and adaptive protection during phase-to-phase faults.

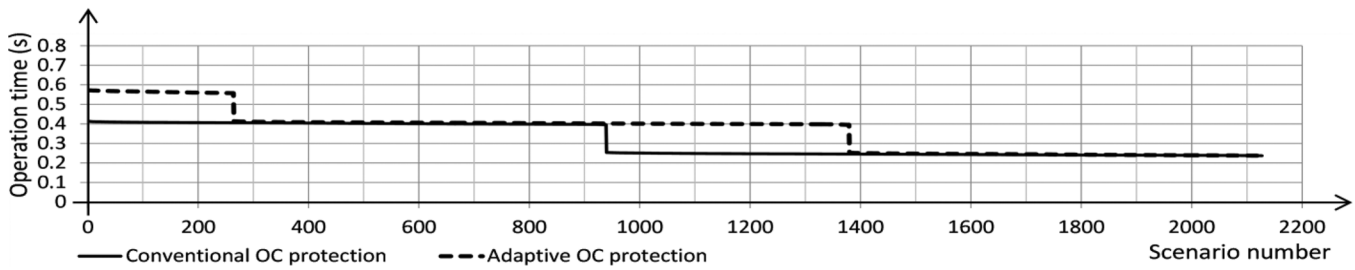

Fig. 8. Measured operating time of conventional and adaptive protection during phase-to-earth faults.

TABLE II
PROTECTION SETTINGS NETWORK SCENARIO 1

	IDMT Phase OC			DTL Phase OC		Earth DTL OC	
	CH	Iset	TMS	Iset	DTL	Iset	DTL
AR-A	SI	400	0.16	1000	0.32	30	0.32
PMAR-A	SI	250	0.1	625	0.16	30	0.16
AR-B	SI	350	0.2	875	0.32	30	0.32
PMAR-B	SI	220	0.1	550	0.16	30	0.16
AR-C	SI	300	0.28	750	0.32	30	0.32
PMAR-C	SI	180	0.1	450	0.16	30	0.16

TABLE III
PROTECTION SETTINGS NETWORK SCENARIO 3

	IDMT Phase OC			DTL Phase OC		Earth DTL OC	
	CH	Iset	TMS	Iset	DTL	Iset	DTL
AR-A	SI	400	**0.17**	1000	**0.48**	30	**0.48**
PMAR-A	SI	250	**0.12**	625	**0.32**	30	**0.32**
AR-B	SI	**250**	**0.1**	**625**	**0.16**	30	**0.16**
PMAR-B	SI	**160**	0.1	**400**	0.16	30	0.16
AR-C	SI	300	0.28	750	0.32	30	0.32
PMAR-C	SI	180	0.1	450	0.16	30	0.16

The analysis of the results revealed that the adaptive overcurrent protection system has improved selectivity and sensitivity with respect to conventional overcurrent protection, for example, when the network topology is changed. It also provides improved coordination with the DG interface protection compared to conventional overcurrent protection. Selected cases will be presented to demonstrate some of these advantages.

A. Impact of Network Automation

Considering scenarios 1 and 3 in Table I, when the network switches from one scenario to another, the adaptive overcurrent protection system calculates the protection settings for the new scenario and applies them to the OCRs. Tables II and III report the automatically calculated protection settings for the two scenarios.

The difference between scenario 1 and scenario 3 is the change of network configuration, that is, the fact that the NOP shifts from S3 to S4. The change of network topology affects the fault current magnitude and path in case of faults in feeders A and B. The new protection settings are therefore different for OCRs AR-A, PMAR-A, AR-B, and PMAR-B as can be observed by comparing Tables II and III. The numbers in bold indicate the modified protection settings.

Without the developed adaptive protection system, that is, using fixed protection settings, the operation speed and correct selectivity of the overcurrent protection system are affected. For example, a 0 Ω phase-to-phase fault between PMAR-B and S4 (fault 6 in Fig. 6) causes the operation of PMAR-A and PMAR-B, as shown in Fig. 9, which causes the unnecessary disconnection of all loads connected between PMAR-A and PMAR-B. With the adaptive system, the problem of miscoordination between PMAR-A and PMAR-B is solved in this particular example, as shown in Fig. 10.

When considering the complete population of simulated faults, it is clear that the instances of false tripping have been reduced from 4.72% to 1.61% (improved security).

B. Impact of DG

Consider scenario 5 in Table I. DG1, DG2, DG3, and DG4 are connected to the network. The presence of DG increases the fault level, changes the magnitudes and paths of fault currents, and, therefore, may cause false tripping and affect the coordination between OCRs.

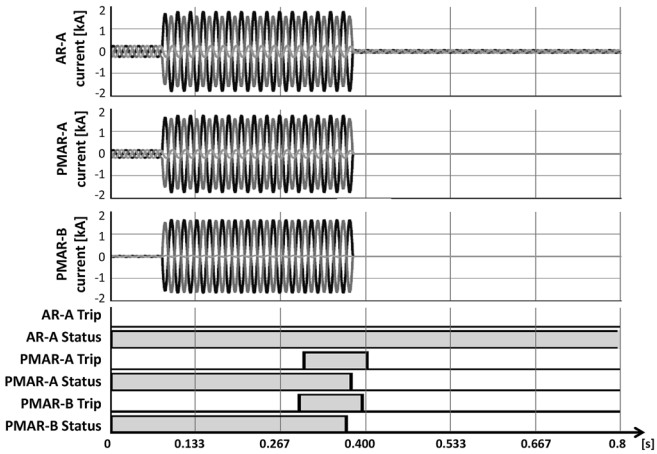

Fig. 9. Fault 6 in scenario 3 without adaptive overcurrent protection.

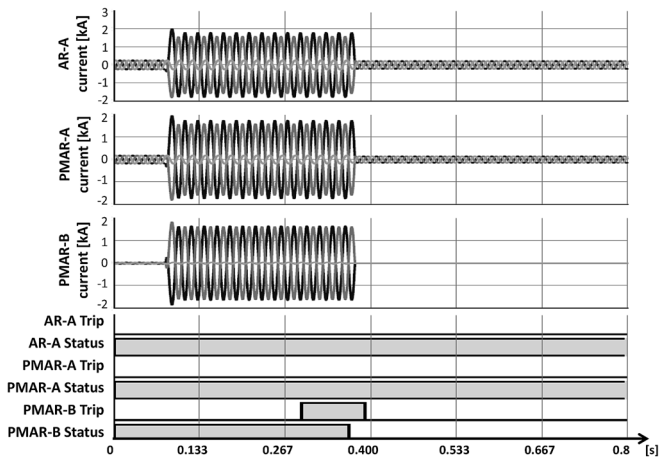

Fig. 10. Fault 6 in scenario 3 with adaptive overcurrent protection.

An example of false tripping is when, in scenario 5, there is a fault on feeder B (fault 4) and the AR-A trips simultaneously with AR-B. This is due to the fault current contribution of DG1 and DG2 to fault 5 and this situation is typical when DNOs adopt DTL instead of IDMT overcurrent protection. To overcome this issue, the protection settings calculated by the overcurrent protection software and presented in Tables II–IV are based on IDMT overcurrent protection plus DTL overcurrent protection for relatively higher fault currents. The DTL pickup current for the protection on each feeder is higher than the total fault current contributions from DGs on the protected feeders to faults located in adjacent feeders.

Another example of false tripping is due to incorrect overload tripping of OCRs. This occurs with traditional overcurrent protection when the network topology is changed and DG creates a load flow that is higher than the tripping current of an OCR. For example, if the network switches to scenario 8, all DG units are connected to feeder 1 and with fixed protection settings may cause false tripping of PMAR-A. By automatically adapting the protection settings (within the thermal limits of the network), that is, increasing the pickup current of PMAR-A to be higher than the sum of the maximum generation from DG2, DG3, and DG4, the problem of false tripping may be overcome.

TABLE IV
PROTECTION SETTINGS NETWORK SCENARIO 13

		IDMT Phase OC		DTL Phase OC		Earth DTL OC	
	CH	Iset	TMS	Iset	DTL	Iset	DTL
AR-A	SI	**240**	**0.12**	**600**	0.32	30	0.32
PMAR-A	SI	**150**	0.1	**375**	0.16	30	0.16
AR-B	SI	**210**	**0.18**	**525**	0.32	30	0.32
PMAR-B	SI	**130**	0.1	**325**	0.16	30	0.16
AR-C	SI	**180**	**0.19**	**450**	0.32	30	0.32
PMAR-C	SI	**100**	0.1	**250**	0.16	30	0.16

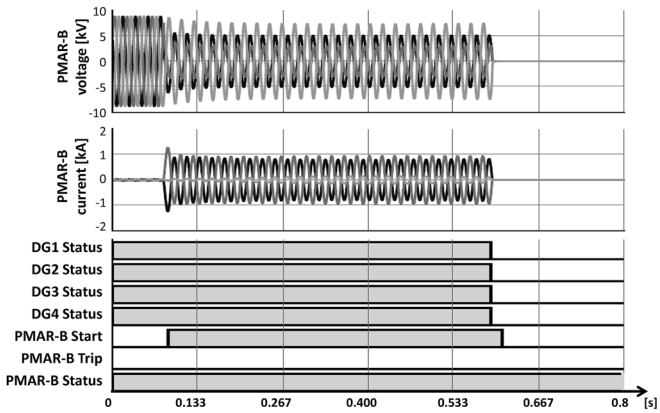

Fig. 11. Fault 8 in scenario 13 without adaptive overcurrent protection.

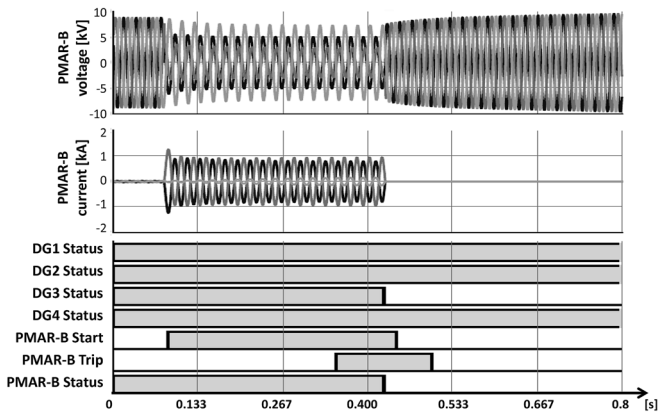

Fig. 12. Fault 8 in scenario 13 with adaptive overcurrent protection.

C. Impact of Islanded Operation

Considering the case when the network changes from grid connected to islanded operation, the fault level changes significantly. For example, from scenarios 1–10 in Table I, the fault level at the 11-kV busbar decreases from 6.8 to 1.7 kA, affecting speed and sensitivity of the protection, potentially leading to slow or even nonoperation during a fault. This may lead to disconnection of the DG supplying the network due to DG interface protection operation.

Dependability of the protection system can be improved in this case by the appropriate adaptation of settings. For example, for a fault downstream of PMAR-B, fault 8, in scenario 10, the standard overcurrent protection system is too slow as shown in

Fig. 11 and, therefore, the DG interface protection trips before the overcurrent protection system isolates the faulted zone.

In the simulation, the interface of the DG has been configured with protection using the settings defined in G59/2 [22]. Fig. 11 shows that the undervoltage protection trips the DG units after 0.5 s.

Simulating the same fault, but with the developed adaptive overcurrent protection system (which changes the protection settings to the values reported in Table IV as soon as the network changes configuration), the overcurrent protection operation is faster as shown in Fig. 11. With the overcurrent protection operating faster, the voltage sags have a shorter duration (as shown in Fig. 12) and DG1, DG2, and DG3 are not disconnected, but continue to supply the loads.

VI. Conclusion

It is clear that the widespread introduction of DG and ANM schemes and the potential for islanded operation of networks in the future will present significant challenges to existing network protection. This paper has illustrated how an adaptive protection scheme can act to address many of these problems and has demonstrated its implementation using a realistic model of an actual distribution network with commercially available hardware and communication schemes.

The novelty of the adaptive overcurrent protection system proposed in this paper is in its algorithm, which differs from other adaptive protection solutions presented in the literature in terms of its possession of higher flexibility and comprehensive coverage of all events that may influence the behavior of the protection system. The algorithm has been explained in detail, focusing on the protection settings calculation technique and the protection system-response evaluation.

The proposed adaptive protection solution is more flexible with respect to other solutions presented in the literature, which are largely based on precalculated protection settings and settings groups. The limitations of using setting groups with precalculated settings is overcome by calculating the optimal protection settings in real time and applying them, after verification of their effectiveness using model-based performance evaluation, to the OCRs when the network status changes.

References

[1] P. P. Barker and R. W. De Mello, "Determining the impact of distributed generation on power systems. I. Radial distribution systems," in *Proc. IEEE Power Eng. Soc. Summer Meeting*, 2000, pp. 1645–1656.

[2] J. Mutale, "Benefits of active management of distribution networks with distributed generation," in *Proc. IEEE Power Eng. Soc. Power Syst. Conf. Expo.*, 2006, pp. 601–606.

[3] J. C. Gomez and M. M. Morcos, "Distributed generation: Exploitation of islanding operation advantages," presented at the Transm. Distrib. Conf. Expo.: Latin America, Bogota, Spain, 2008.

[4] A. A. Chowdhury, D. O. Koval, and S. M. Islam, "Islanding operation of distributed generators in active distribution networks," presented at the 43rd Int. Univ. Power Eng. Conf., Sydney, Australia, 2008.

[5] C. Mozina, "Impact of green power distributed generation," *IEEE Ind. Appl. Mag.*, vol. 16, no. 4, pp. 55–62, Jul./Aug. 2010.

[6] K. Kauhaniemi and L. Kumpulainen, "Impact of distributed generation on the protection of distribution networks," in *Proc. 8th Inst. Elect. Eng. Int. Conf. Develop. Power Syst. Protect.*, 2004, pp. 315–318.

[7] A. Girgis and S. Brahma, "Effect of distributed generation on protective device coordination in distribution system," in *Proc. Large Eng. Syst. Conf. Power Eng.*, 2001, pp. 115–119.

[8] K. L. Butler-Purry and M. Marotti, "Impact of distributed generators on protective devices in radial distribution systems," in *Proc. IEEE Power Eng. Soc. Transm. Distrib. Conf. Exhibit.*, 2006, pp. 87–88.

[9] M. S. Sachdev, T. S. Sidhu, and B. K. Talukdar, "Topology detection for adaptive protection of distribution networks," in *Proc. Int. Conf. Energy Manage. Power Del.*, 1995, pp. 445–450.

[10] P. Mahat, C. Zhe, B. Bak-Jensen, and C. L. Bak, "A simple adaptive overcurrent protection of distribution systems with distributed generation," *IEEE Trans. Smart Grid*, vol. 2, no. 3, pp. 428–437, Sep. 2011.

[11] I. Chilvers, N. Jenkins, and P. Crossley, "Distance relaying of 11 kV circuits to increase the installed capacity of distributed generation," *Proc. Inst. Elect. Eng., Gen., Transm. Distrib.*, vol. 152, pp. 40–46, 2005.

[12] G. Tang and M. R. Iravani, "Application of a fault current limiter to minimize distributed generation impact on coordinated relay protection," presented at the Int. Conf. Power Syst. Transients, Montreal, QC, Canada, 2005.

[13] A. Agheli, H. A. Abyaneh, R. M. Chabanloo, and H. H. Dezaki, "Reducing the impact of DG in distribution networks protection using fault current limiters," in *Proc.4th Int. Power Eng. Optimiz. Conf.*, 2010, pp. 298–303.

[14] W. El-khattam and T. S. Sidhu, "Resolving the impact of distributed renewable generation on directional overcurrent relay coordination: A case study," *IET Renew. Power Gen.*, vol. 3, pp. 415–425, 2009.

[15] M. Baran and I. El-Markabi, "Adaptive over current protection for distribution feeders with distributed generators," in *Proc. IEEE Power Eng. Soc. Power Syst. Conf. Expo.*, 2004, pp. 715–719.

[16] N. Schaefer, T. Degner, A. Shustov, T. Keil, and J. Jaeger, "Adaptive protection system for distribution networks with distributed energy resources," presented at the 10th IET Int. Conf. Develop. Power Syst. Protect., Manchester, U.K., 2010.

[17] H. Cheung, A. Hamlyn, Y. Cungang, and R. Cheung, "Network-based adaptive protection strategy for feeders with distributed generations," in *Proc. IEEE Canada Elect. Power Conf.*, 2007, pp. 514–519.

[18] I. Abdulhadi, F. Coffele, A. Dysko, C. Booth, and G. Burt, "Adaptive protection architecture for the smart grid," in *Proc. 2nd IEEE Power Eng. Soc. Int. Conf. Exhibit. Innovative Smart Grid Technol.*, 2011, pp. 1–8.

[19] Python Software 2.7. Python, Oct. 1, 2012. [Online]. Available: http://www.python.org

[20] IPSA Power Software. TNEI., Oct. 1, 2012. [Online]. Available: http://www.ipsa-power.com/software

[21] DTI, United Kingdom Generic Distribution System (UKGDS). 2005. [Online]. Available: http://www.sedg.ac.uk/

[22] Recommendations for the connection of generating plant to the distribution systems of licensed distribution network operators, ENA Engineering Recommendation G59/2. 2010.

F. Coffele received the B.Eng. and M.Eng. degrees in electrical engineering from the University of Padova, Padova, Italy, in 2004 and 2007, respectively, and the Ph.D. degree in electronic and electrical engineering from the University of Strathclyde, Glasgow, U.K., in 2012.

Currently, he is the Research and Development Manager of the Power Network Demonstration Centre, University of Strathclyde, Glasgow, U.K. His research interests include power system protection, automation, and control.

C. Booth received the B.Eng. (Hons.) and Ph.D. degrees in Electronic and Electrical Engineering from the University of Strathclyde, Glasgow, U.K., in 1991 and 1996, respectively

Currently, he is a Senior Lecturer within the Institute for Energy and Environment, University of Strathclyde, Glasgow, U.K. His research interests include power system protection and plant condition monitoring.

A. Dyśko (M'06) received the M.Sc. degree in electronic and electrical engineering from the Technical University of Łódź, Łódź, Poland, in 1990, and the Ph.D. degree in electronic and electrical engineering from the University of Strathclyde, Glasgow, U.K., in 1998.

Currently, he is a Lecturer in the Department of Electronic and Electrical Engineering, University of Strathclyde. His main interest areas are power system modeling, protection, and power quality.